

A STOCHASTIC METHOD FOR SOLVING TIME-FRACTIONAL DIFFERENTIAL EQUATIONS*

NICOLAS L. GUIDOTTI[†], JUAN A. ACEBRÓN[‡], AND JOSÉ MONTEIRO[†]

Abstract. We present a stochastic method for efficiently computing the solution of time-fractional partial differential equations (fpDEs) that model anomalous diffusion problems of the subdiffusive type. After discretizing the fpDE in space, the ensuing system of fractional linear equations is solved resorting to a Monte Carlo evaluation of the corresponding Mittag-Leffler matrix function. This is accomplished through the approximation of the expected value of a suitable multiplicative functional of a stochastic process, which consists of a Markov chain whose sojourn times in every state are Mittag-Leffler distributed. The resulting algorithm is able to calculate the solution at conveniently chosen points in the domain with high efficiency. In addition, we present how to generalize this algorithm in order to compute the complete solution. For several large-scale numerical problems, our method showed remarkable performance in both shared-memory and distributed-memory systems, achieving nearly perfect scalability up to 16,384 CPU cores.

Key words. Monte Carlo method, time-fractional differential equations, anomalous diffusion, Mittag-Leffler function, matrix functions, parallel algorithms, high performance computing

MSC codes. 33E12, 35R11, 60K50, 65C05, 68W10

1. Introduction. Among the many non-conventional statistical phenomena observed experimentally in the last few years and characterized typically by unusual scaling exponents, the anomalous diffusion stands out for its major impact in a variety of scientific disciplines [42]. To cite just a few relevant examples, it has been already observed in turbulent atmosphere, transport in amorphous solids, diffusion in cell nucleus, magnetic resonance imaging, search behavior, and in finance for an accurate modeling of the stock price fluctuations.

In the anomalous diffusion, the mean squared displacement (MSD) vary nonlinearly in time, *i.e.*, $\langle x^2(t) \rangle \sim t^\alpha$ with $\alpha \neq 1$, during the entire process. Here $x(t)$ is the relative position at time t of a particle with respect to a given reference point. This contrasts with the classical diffusion problems, modeled typically by a Brownian motion, where it is well known that the MSD grows linearly in time. In practice, there are two different types of regimes according to the value of the scaling exponent α . The phenomenon is termed as subdiffusion when $\alpha < 1$ and, superdiffusion when $\alpha > 1$. It has been proposed in the literature several pathways leading to anomalous diffusion. The most commonly found are the presence of long-range correlations, non-identical displacements, or non-finite mean or variance of the probability density function for the trajectory displacements.

Within this context, fractional calculus has been proven to be extremely useful in order to provide realistic models for many real-life processes and phenomena [54, 36]. The main reason for this is due to fractional derivative operators being in practice non-local operators, and therefore they are specially suited for describing the long-time

*Submitted to the editors in 28/03/2023.

Funding: This work was supported by Fundação para a Ciência e a Tecnologia under grant 2022.11506.BD and projects UIDB/50021/2020, 2022.08838.PTDC and PTDC/CCI-INF/6762/2020. JA was funded by Ministerio de Universidades and specifically the requalification program of the Spanish University System 2021-2023 at the Carlos III University.

[†]INESC-ID, Instituto Superior Técnico, Universidade de Lisboa, Portugal (nicolas.guidotti@tecnico.ulisboa.pt, jcm@inesc-id.pt).

[‡]Department of Mathematics, Carlos III University of Madrid, Spain (juan.acebron@tecnico.ulisboa.pt).

memory and spatial heterogeneity effects typically found in any anomalous diffusion problem.

The formal solution to the simplest dynamical problem defined by a system of linear fractional rate equations for an n -dimensional process $\mathbf{y}(t)$ subject to a given initial condition $\mathbf{y}(0) = \mathbf{y}_0$ is

$$(1.1) \quad \mathbf{y}(t) = E_\alpha(\mathbf{A} t^\alpha) \mathbf{y}_0,$$

where \mathbf{A} is an $n \times n$ matrix of constant coefficients. When $\alpha = 1$, the Mittag-Leffler (ML) function $E_\alpha(\mathbf{A} t^\alpha)$ reduces to the matrix exponential $e^{\mathbf{A} t}$. The ML function also appears in other scientific domains, such as biology [13, 37], physics [26, 49, 38], control systems [49, 7] and complex network analysis [4, 41]. It is important to remark here that this system of linear rate equations serve as building-blocks for more complex systems, and therefore becomes of paramount importance investigating algorithms capable of computing it efficiently.

However, an efficient algorithm for solving large-scale problems is still missing. Therefore, the main contribution of this paper is to propose a probabilistic method for the efficient computation of the ML matrix function. This method is based on random walks that change states according to a suitable continuous-time Markov chain, whose sojourn times follows a Mittag-Leffler distribution. Such method allows us to compute the ML matrix function for large-scale matrices, focusing primarily here on the action of the function over a vector. Our second contribution is an extensive analysis of the performance and convergence of our method using a few relevant numerical examples, including a formal description of the variance and a performance comparison against classical algorithms. Our third and last contribution was to parallelize and analyze the scalability of the stochastic algorithm for a large number of processors (up to 16,384 CPU cores) in the Karolina Supercomputer located in IT4Innovations National Supercomputing Centre.

The paper is organized as follows. In the next section we give an overview of the state of the art in this area. Section 3 describes the probabilistic method and its practical implementation. This section also shows how a program can generate random numbers from the Mittag-Leffler probability distribution. In Section 4, several numerical experiments are presented in order to characterize the performance and numerical errors of the stochastic method compared to classical approaches. Finally, in Section 5, we highlight the main results and conclude the paper.

2. Background. One of the major drawbacks of describing a problem in terms of fractional operators is the lack of uniqueness in the mathematical formulation. This contrasts sharply with the classical calculus. In fact, in fractional calculus there exists a variety of different definitions of fractional operators (differentials and integrals), and they are chosen according to a given set of assumptions imposed to satisfy different needs and constraints of the particular problem. There are already in the literature a number of excellent texts that review the mathematics of fractional calculus, *e.g.* [38]. Among the different definitions of fractional operators, the Caputo fractional derivative appears as the most commonly used for modeling temporal evolution phenomena, which accounts for past interactions and also non-local properties. Moreover, mathematically the initial conditions imposed for fractional differential equations with Caputo derivatives coincides with the integer-order differential equations. Such derivative is defined as follows:

$$(2.1) \quad {}^C D_t^\alpha f(t) = \int_0^t \frac{f^{(n)}(\tau)}{(t-\tau)^{\alpha+1-n}} d\tau$$

with n an integer such that $n = \lceil \alpha \rceil$. Note that if $0 < \alpha < 1$, $n = 1$.

The simplest dynamical process described in terms of fractional operators consists in an initial value problem for a linear fractional rate equation, which for a given variable $y(t)$ is given by

$$(2.2) \quad {}^C D_t^\alpha y(t) = -\lambda y(t), \quad y(0) = y_0.$$

The solution of this equation can not be expressed in a closed-form, being rather an infinite series. It was first obtained by the mathematician Mittag-Leffler, and is formally written as

$$(2.3) \quad y(t) = y_0 E_\alpha(-\lambda t^\alpha),$$

where $E_\alpha(t)$ is the function defined as

$$(2.4) \quad E_\alpha(-\lambda t^\alpha) = \sum_{k=0}^{\infty} \frac{(-\lambda t^\alpha)^k}{\Gamma(k\alpha + 1)},$$

and carries his name. Here $\Gamma(x)$ denotes the Euclidean Gamma function. Note that when $\alpha = 1$, it reduces to the exponential function. Essentially, the Mittag-Leffler function generalizes the exponential function, and has been considered for many as the *Queen function* of the fractional calculus [39, 19, 21]. For complex parameters α and β with $\Re\{\alpha\} > 0$, the Mittag-Leffler function (ML function) can be further generalized, and was defined as

$$(2.5) \quad E_{\alpha,\beta}(z) = \sum_{k=0}^{\infty} \frac{z^k}{\Gamma(k\alpha + \beta)}, z \in \mathbb{C}.$$

Here $E_{\alpha,\beta}(z)$ is an entire function of order $\rho = 1/\Re\{\alpha\}$ and type 1. The exponential function can be recovered by setting $\alpha = \beta = 1$ since $\Gamma(k + 1) = k!$ for $k \in \mathbb{N}$. When $\beta = 1$, the notation of the ML function can be simplified to $E_\alpha(z) = E_{\alpha,1}(z)$.

In this paper we consider the n -dimensional case of a system described by a set time-fractional linear differential equations, whose solution is given by (1.1). We therefore need to evaluate the ML function over a potentially very large system's matrix.

A naive approach to evaluate the ML function comes directly from its definition in (2.5). However, this is ill-advised for most applications since the convergence of the series is very slow if either the modulus $|z|$ is large or the value of α is small. Moreover, the terms of the series may grow very large before decreasing, which can cause overflows and catastrophic numerical cancellations when using standard double-precision arithmetic (IEEE 754). For this reason, the scalar ML function is usually evaluated through alternative methods [27, 16, 51, 20], such as the Taylor series, inversion of the Laplace transformation, integral representation and other techniques.

To evaluate the ML matrix function, Garrappa [17] recently proposed a Schur-Parlett algorithm [8], which in practice requires computing its derivatives. This method, however, is only suited for small matrices since the Schur-Parlett algorithm scales with $O(n^3)$, but it can go up to $O(n^4)$ depending on the distribution of the eigenvalues. Moreover, if the eigenvalues are highly clustered, the algorithm may require high-order derivatives which are more expensive to compute, while also being less accurate. There is also a Krylov-based method for computing the action of a Mittag-Leffler function over a vector [43], however, the code is not publicly available.

As an alternative to deterministic methods, Monte Carlo algorithms for approximating matrix functions have already been proposed in the past [14, 10, 11, 29, 5], primarily for solving linear systems. The main idea of these algorithms consists in generating random paths corresponding to the realizations of a discrete Markov chain. Those random paths evolve through the different indices of the matrix \mathbf{A} , which is used as the generator. Essentially, the method corresponds to a Monte Carlo sampling of the Neumann series [25] of the matrix. The convergence of this method was rigorously established in [5, 29, 12]. It is broadly accepted that these stochastic methods offer interesting features from a computational point of view, such as being easily parallelizable, fault-tolerant, and more suited to heterogeneous architectures (which are extremely important attributes in view of the current high performance computers). However, the truth is that they also exhibit some significant weaknesses, namely a very slow convergence rate to the solution. This can cause the underlying algorithms to be highly demanding computationally, especially when high accuracy solutions are required.

The extension of the Monte Carlo method for other matrix functions, such as the matrix exponential, was only accomplished recently in [2]. The method consists in generating continuous-time random walks over the matrix \mathbf{A} , whose holding time follows an exponential distribution. Later, [3] applied a multilevel technique to improve the performance of this method.

For the specific case of the one-dimensional fractional diffusion equation, [44] introduced a Monte Carlo method for simulating discrete time random walks which are used for obtaining numerical solutions of the fractional equation, but not for computing the ML matrix function.

3. Description of the Probabilistic Method. In this section, we describe the probabilistic representation of the solution vector as well as a practical algorithm for approximating the action of the Mittag-Leffler function over a vector using this representation. With slight modifications, the algorithm can either calculate a single entry of the solution vector or the full solution. We also present a way to sample random numbers from the Mittag-Leffler distribution.

3.1. Mathematical description. Consider: $\mathbf{A} = (a_{ij})$, a general n -by- n matrix with $a_{ii} < 0 \forall i$; \mathbf{u} , a given n -dimensional vector; and \mathbf{y} , an n -dimensional vector. This last vector corresponds to the solution vector after computing the action of the Mittag-Leffler function over the vector \mathbf{u} , that is $\mathbf{y} = E_{\alpha,\beta}(\mathbf{A} t^\alpha) \mathbf{u}$ with $0 < \alpha \leq 1$, $\beta > 0$ and $t \geq 0$. Here t denotes the value of time when the solution is computed.

Let us define the following matrices: a diagonal matrix \mathbf{D} , represented hereafter as a vector \mathbf{d} , with entries $d_{ij} = 0$ for $\forall i \neq j$ and $d_{ii} = d_i = a_{ii}$ for $i = 1, \dots, n$; \mathbf{M} , a matrix obtained as $\mathbf{M} = \mathbf{A} - \mathbf{D}$, and hence with zero diagonal entries; \mathbf{Q} , the matrix with entries q_{ij} given by

$$(3.1) \quad q_{ij} = \begin{cases} 0, & \text{if } i = j \\ \frac{|m_{ij}|}{\sum_{j=1}^n |m_{ij}|}, & \text{otherwise;} \end{cases}$$

\mathbf{G} , a matrix with entries g_{ij} taking values 1 when $m_{ij} \geq 0$, and -1 otherwise; and finally \mathbf{R} , a matrix with entries

$$(3.2) \quad r_{ij} = \begin{cases} r_i = \frac{\sum_{j=1}^n |m_{ij}|}{d_i}, & \text{if } i = j \\ 0, & \text{otherwise;} \end{cases}$$

Note that $\sum_{j=1}^n q_{ij} = 1 \quad \forall i$, and therefore matrix \mathbf{Q} can be used as the transition rate matrix of a given Markov chain. Furthermore, it holds that $\mathbf{M} = \mathbf{D} \mathbf{R} (\mathbf{G} * \mathbf{Q})$, where $*$ denotes element-wise matrix multiplication.

THEOREM 3.1. *Let $\{X_t : t \geq 0\}$ be a stochastic process with finite state space $\Omega = \{1, 2, \dots, n\}$ given by*

$$(3.3) \quad X_t = \sum_{m=1}^{\infty} Z_{m-1} \mathbf{1}_{[T_{m-1} \leq t \leq T_m]}.$$

Such process changes states according to a Markov chain $Z = (Z_m)_{m \in \mathbb{N}}$, which takes values in Ω and \mathbf{Q} is the corresponding transition matrix. Here, T_k is the time of the k -th event, and $\mathbf{1}_E$ denotes the indicator function, being 1 or 0 depending on whether the event E occurs. The sojourn times in the i -th state follow the Mittag-Leffler distribution $ML_{\alpha}(d_i)$. Then, we have that any entry i of the solution vector \mathbf{y} can be represented probabilistically as

$$(3.4) \quad y_i = \mathbb{E} \left[u_{X_0} \mathbf{1}_{[T_0 > t]} + \left(\prod_{j=1}^{\eta} r_{X_{T_{j-1}}} g_{X_{T_{j-1}}, X_{T_j}} \right) u_{X_{T_{\eta}}} \mathbf{1}_{[T_0 \leq t]} \right],$$

where $X_0 = i$. Here \mathbb{E} is the expected value with respect to the joint distribution function of the random variables T and η , where η is the number of events occurring between 0 and t .

Proof. Our goal is to prove that the expected value of the functional of the stochastic process X_t in (3.4) coincides with the vector solution \mathbf{y} . As a first step in the proof, it is required to compute the joint distribution function of the random variables T and η . This function depends on the probability of jumping from state i to state j at time t , $\mathbb{P}(X_t = j | X_0 = i)$. Let us define \mathbf{P} as the probability matrix such that $\mathbf{P}(t) = (p_{ij}) = \mathbb{P}(X_t = j | X_0 = i)$, then it holds that

$$(3.5) \quad p_{ij}(t) = \delta_{ij} \mathbb{P}(t_i > t) + \int_0^t ds f_i(s) \sum_{l \neq i} \mathbb{P}(X_{\tau} = l, X_t = j | \tau = s),$$

where t_i corresponds to the instant of time of a first event when the state is i . Here the function $f_i(s) = -d_i s^{\alpha-1} E_{\alpha, \alpha}(d_i s^{\alpha})$ is a density function. In fact, it satisfies that

$$(3.6) \quad \int_0^{\infty} ds f_i(s) = 1,$$

and is called the Mittag-Leffler density function [19]. Then the probability of no events taking place in the interval of time $[0, t]$, $\mathbb{P}(t_i > t)$, is given by

$$(3.7) \quad \mathbb{P}(t_i > t) = \int_t^{\infty} ds f_i(s) = E_{\alpha}(d_i t^{\alpha}).$$

Therefore, it follows that

$$(3.8) \quad p_{ij}(t) = \delta_{ij} E_{\alpha}(d_i t^{\alpha}) + \int_0^t ds f_i(s) \sum_{l \neq i} q_{il} p_{lj}(t-s).$$

This is an integral equation for $p_{ij}(t)$ that can be solved recursively, and the solution can be rewritten formally as

$$(3.9) \quad p_{ij}(t) = \sum_{\eta=0}^{\infty} p_{ij}^{(\eta)}(t),$$

where $p_{ij}^{(\eta)}(t)$ denotes the probability of having a transition from i to j when η events occur during the time interval $[0, t]$. Let $\nu_i^{(\eta)}$ be the corresponding contribution to the solution y_i for η events. If no events occur, the contribution to the solution $\nu_i^{(0)}$ can be readily obtained as $E_\alpha(d_i t^\alpha) u_i$. The remaining contributions can be obtained as follows. For one event, from (3.8) the probability is given by

$$(3.10) \quad p_{ij}^{(1)}(t) = \int_0^t ds f_i(s) \sum_{l \neq i} q_{il} \delta_{lj} E_\alpha(d_l (t-s)^\alpha),$$

and thus the corresponding contribution to the solution is

$$(3.11) \quad \nu_i^{(1)} = \sum_{j=1}^n \int_0^t ds f_i(s) \sum_{l \neq i} r_i g_{il} q_{il} \delta_{lj} E_\alpha(d_l (t-s)^\alpha) u_j.$$

Note that the equation above can be rewritten equivalently in matrix form as

$$(3.12) \quad \boldsymbol{\nu}^{(1)} = \int_0^t ds \mathbf{f}(s) \mathbf{R} (\mathbf{G} * \mathbf{Q}) E_\alpha(\mathbf{D} (t-s)^\alpha) \mathbf{u},$$

where $\boldsymbol{\nu}^{(1)}$ and $\mathbf{f}(s)$ are vectors with components $\nu_i^{(1)}$ and $f_i(s)$, respectively. Since $\mathbf{R} (\mathbf{G} * \mathbf{Q}) = \mathbf{D}^{-1} \mathbf{M}$, then

$$(3.13) \quad \boldsymbol{\nu}^{(1)} = - \int_0^t ds s^{\alpha-1} E_{\alpha, \alpha}(\mathbf{D} s^\alpha) \mathbf{M} E_\alpha(\mathbf{D} (t-s)^\alpha) \mathbf{u}.$$

The contribution corresponding to two events is

$$(3.14) \quad \boldsymbol{\nu}^{(2)} = \int_0^t ds_1 \mathbf{f}(s_1) \mathbf{D}^{-1} \mathbf{M} \int_0^{t-s_1} ds_2 \mathbf{f}(s_2) \mathbf{D}^{-1} \mathbf{M} E_\alpha(\mathbf{D} (t-s_1-s_2)^\alpha) \mathbf{u}.$$

For arbitrary number of events η , the contribution can be readily computed, and written compactly as follows

$$(3.15) \quad \boldsymbol{\nu}^{(\eta)} = (-1)^\eta \mathbf{H}^\eta E_\alpha(\mathbf{D} t) \mathbf{u}, \quad \forall \eta \geq 0.$$

Here \mathbf{H} is an integral operator \mathbf{H} defined as

$$(3.16) \quad \mathbf{H}\psi(t) := \int_0^t ds \mathbf{f}(s) \mathbf{D}^{-1} \mathbf{M} \psi(t-s).$$

The solution \mathbf{y} is finally obtained summing all those partial contributions, and yields

$$(3.17) \quad \mathbf{y} = \sum_{\eta=0}^{\infty} \boldsymbol{\nu}^{(\eta)} = (\mathbf{I} + \mathbf{H})^{-1} E_\alpha(\mathbf{D} t) \mathbf{u},$$

which can be expressed equivalently as an integral equation in the form

$$(3.18) \quad \mathbf{y} = E_\alpha(\mathbf{D}t) \mathbf{u} - \int_0^t ds \mathbf{f}(s) \mathbf{D}^{-1} \mathbf{M} \mathbf{y}(t-s).$$

Taking the Laplace transform, and using that [19]

$$(3.19) \quad \mathcal{L}\{t^{\beta-1} E_{\alpha,\beta}(ct^\alpha)\} = s^{-\beta}(1 - cs^{-\alpha})^{-1},$$

we obtain

$$(3.20) \quad \hat{\mathbf{y}}(s) = \frac{s^{-1}}{\mathbf{I} - \mathbf{D} s^{-\alpha}} \mathbf{u} + \frac{\mathbf{D} s^{-\alpha}}{\mathbf{I} - \mathbf{D} s^{-\alpha}} \mathbf{D}^{-1} \mathbf{M} \hat{\mathbf{y}},$$

where $\hat{\mathbf{y}}(s) = \mathcal{L}\{y(t)\}$. The solution is

$$(3.21) \quad \hat{\mathbf{y}} = \frac{s^{-1}}{\mathbf{I} - \mathbf{D} s^{-\alpha} - \mathbf{D} s^{-\alpha} \mathbf{D}^{-1} \mathbf{M}} \mathbf{u}.$$

After applying the inverse Laplace transform and using again (3.19), we obtain

$$(3.22) \quad \mathbf{y} = E_\alpha((\mathbf{D} + \mathbf{M})t^\alpha) \mathbf{u} = E_\alpha(\mathbf{A}t^\alpha) \mathbf{u},$$

which concludes the proof. \square

3.2. Implementation. According to Theorem 3.1, the value of the i -th entry of the solution vector \mathbf{y} can be estimated through the simulation of the stochastic process X_t , which consists in generating random paths from the Markov chain Z and then computing the realization of a random variable ω over these paths. Each random path starts at state X_0 and time $\tau = 0$ and then jumps from one state to the next until it reaches the time $\tau = t$. The next state is always selected at random based on the transition matrix \mathbf{Q} and the sojourn time in each state follows an ML distribution. For a sequence of states X_0, X_1, \dots, X_η , the value of ω associated with this random path can be calculated as

$$\omega = \left(\prod_{j=1}^{\eta} r_{X_{j-1}} g_{X_{j-1}, X_j} \right) u_{X_\eta}$$

The procedure for simulating the process X_t is described in Algorithm 3.1. In order for the computation to be practical, Algorithm 3.1 can only generate a finite number N_p of random paths and approximate the value of y_i as

$$(3.23) \quad y_i \approx \frac{1}{N_p} \sum_{j=1}^{N_p} \omega_j$$

where ω_j is the realization of ω over the random path j . Naturally, replacing the expected value in (3.4) by the arithmetic mean over a finite sample size N_p in (3.23) leads to a numerical error ϵ of order of $O(N_p^{-1/2})$. In fact, it is well-known that the arithmetic mean provides the best unbiased estimator for the expected value, and, for large number N_p of random paths, the error ϵ is approximately a random variable distributed according to a normal distribution with standard deviation $\epsilon \approx \sigma N_p^{-1/2}$

Algorithm 3.1 Calculates the i -th entry of $\mathbf{y} = E_\alpha(\mathbf{A} t^\alpha) \mathbf{u}$ based on Theorem 3.1. N_p indicates the number of random paths.

```

1: function MCML_SINGLE( $\mathbf{A}, \mathbf{u}, \alpha, i, N_p, t$ )
2:    $y_i = 0$ 
3:   for each random path do
4:      $X_0 = i; \omega = 1; k = 0$ 
5:     Generate  $Z_\alpha \sim ML_\alpha(d_{X_0})$ 
6:      $\tau = Z_\alpha$ 
7:     while  $\tau < t$  do
8:        $X_{k+1} = \text{SELECTNEXTSTATE}(X_k, \mathbf{Q})$ 
9:        $\omega = \omega \times r_{X_k} g_{X_k, X_{k+1}}$ 
10:      Generate  $Z_\alpha \sim ML_\alpha(d_{X_k})$ 
11:       $\tau = \tau + Z_\alpha$ 
12:       $k = k + 1$ 
13:    end while
14:     $y_i = y_i + \omega u_{X_k}$ 
15:  end for
16:   $y_i = y_i / N_p$ 
17:  return  $y_i$ 
18: end function

```

[6]. Here σ denotes the standard deviation of the random variable ω . Note that there is no other source of error in Algorithm 3.1.

The main limitation of Algorithm 3.1 is that it can only estimate one entry of \mathbf{y} at a time, requiring a separated set of random paths to calculate the solution in each point in the domain. Therefore, it is better suited for estimating the solution locally (*i.e.*, for a specific set of number of points) than the complete solution. A more efficient method for computing the solution for the entire domain is presented next.

3.3. Computing the full solution vector. Theorem 3.1 can be conveniently modified to represent the complete solution vector \mathbf{y} rather than a single entry. The procedure is identical to the case of the matrix exponential (namely $\alpha = \beta = 1$), which is described fully in [3]. For completeness, we present here the main details. The representation requires generating random paths, which now start at a randomly chosen state j and time $t = 0$ according to a suitable distribution probability $p_j^{(0)} = \mathbb{P}(X_0 = j)$, ending at state i at time t . Those paths evolve in time changing states governed now by \mathbf{Q}^\top as the corresponding transition matrix of the Markov chain. This can be explained resorting to the Bayes' theorem. In fact, it holds that

$$\begin{aligned}
p_{ji} &= \mathbb{P}(X_t = i | X_0 = j) \\
&= \mathbb{P}(X_t = j | X_0 = i) \frac{\mathbb{P}(X_t = i)}{\mathbb{P}(X_0 = j)} \\
&= p_{ij} \frac{p_i}{p_j^{(0)}} \\
&= (\mathbf{P}^\top)_{ji} \frac{p_i}{p_j^{(0)}}
\end{aligned}$$

where $p_i = \mathbb{P}(X_t = i)$. Note that the matrix probability (\mathbf{P}^\top) corresponds to a Markov chain governed now by the transition matrix \mathbf{Q}^\top . As it was explained in [3],

Algorithm 3.2 Calculates $\mathbf{y} = E_\alpha(\mathbf{A} t^\alpha) \mathbf{u}$ based on its full probabilistic representation. N_p indicate the number of random paths.

```

1: function MCML_FULL( $\mathbf{A}$ ,  $\mathbf{u}$ ,  $\alpha$ ,  $N_p$ ,  $t$ )
2:    $\mathbf{y} = 0$ 
3:    $\mathbf{p}^{(0)} = \left\{ p_i^{(0)} = \frac{|u_i|}{\|\mathbf{u}\|_1} \right\}$ 
4:   for each random path do
5:      $k = 0$ 
6:      $X_0 = \text{SELECTINITIALSTATE}(\mathbf{p}^{(0)})$ 
7:      $\omega = \frac{u_{X_0}}{|u_{X_0}|} \|\mathbf{u}\|_1$ 
8:     Generate  $Z_\alpha \sim ML_\alpha(d_{X_0})$ 
9:      $\tau = Z_\alpha$ 
10:    while  $\tau < t$  do
11:       $X_{k+1} = \text{SELECTNEXTSTATE}(X_k, \mathbf{Q}^\top)$ 
12:       $\omega = \omega \times r_{X_k} g_{X_k, X_{k+1}}$ 
13:      Generate  $Z_\alpha \sim ML_\alpha(d_{X_k})$ 
14:       $\tau = \tau + Z_\alpha$ 
15:       $k = k + 1$ 
16:    end while
17:     $y_{X_0} = y_{X_0} + \omega$ 
18:  end for
19:   $\mathbf{y} = \mathbf{y}/N_p$ 
20:  return  $\mathbf{y}$ 
21: end function

```

the distribution function $p_j^{(0)}$ can be arbitrarily chosen. However, the choice may have a direct impact on the variance, and, in turn, on the performance of the algorithm. For simplicity, we use here the more reasonable choice corresponding to $p_j^{(0)}$ proportional to $|u_j|$, since this resembles the well known importance sampling method for variance reduction, where the sampling is done according to the importance of the data.

Algorithm 3.2 describes the stochastic method based on this alternative representation. The main advantage of this method is the ability to estimate the entire solution vector with a single set of random paths, naturally distributing the contribution of each random path over all points in the domain. Due to this property, Algorithm 3.2 is often more efficient than Algorithm 3.1 for estimating the entire solution.

3.4. Generating random numbers from a Mittag-Leffler distribution.

For every state in the random path, Algorithms 3.1 and 3.2 generate a random number Z_α from the ML probability distribution to determine the time spent in this state. The value of Z_α is then later added to the total time τ of the random path. The random path ends when $\tau \geq t$.

Considering that an ML random variable follows the Geometric Stable Laws [33, 32], it can be represented as a combination of an exponential and a stable random variable [31, 30]. Using this representation, Kozubowski [30] deducted the following formula for generating $Z_\alpha \sim ML_\alpha(\gamma)$ for $0 < \alpha \leq 1$:

$$(3.24) \quad Z_\alpha = -|\gamma|^{-\frac{1}{\alpha}} \ln(U) [\sin(\alpha\pi) \cot(\alpha\pi V) - \cos(\alpha\pi)]^{\frac{1}{\alpha}}$$

where U, V are random numbers from the uniform distribution over the $[0, 1]$ interval and γ is the rate parameter. For $\alpha = 1$, (3.24) reduces to the inversion formula for the exponential distribution: $Z_1 = -|\gamma|^{-1} \ln U$. Note that for $\alpha > 1$, the ML function is not monotonic and, thus, cannot be considered a probability distribution [47]. It is worth mentioning that the *rejection sampling* technique [9, 40, 48] can also be used for generating the ML random numbers, however it requires the construction of a pointwise representation directly from (2.5), which can be quite expensive due to the slow convergence of the series [15].

4. Numerical Results. In this section, we evaluate the performance of our Monte Carlo method by solving time-fractional partial differential equations (fPDEs) through the method of lines. The method of lines [50, 22] consists in discretizing the spatial variables of the initial problem to obtain a system of coupled fractional ordinary differential equations with time as the independent variable. The system can then be solved by computing the action of the Mittag-Leffler function over the discretized initial values. Using this method, we solve the Dirichlet boundary-value problem for both a 2D time-fractional diffusion equation and a 3D time-fractional convection-diffusion equation.

4.1. Setup. All simulations regarding the shared-memory architecture were executed on a commodity workstation with an AMD Ryzen 5800X 8C @4.7GHz and 32GB of RAM, running Arch Linux. The `MCML_Full` (Algorithm 3.2) was implemented in C++ with OpenMP and uses `PCG64DXSM` [45] as its random number generator. `PCG64DXSM` is an improved version of the default generator of the popular NumPy [23] module for Python. The code was compiled with the Clang/LLVM v14.0.0 with the `-O3` and `-march=znver3` flags. We will refer to the Monte Carlo method that uses dense and sparse matrices as `mc_dense` and `mc_sparse`, respectively.

To the best of our knowledge, the only freely available code capable of computing the Mittag-Leffler function for matrices was proposed by Garrappa and Popolizio [17] and it is written in MATLAB 2021a. This code is based on the Schur-Parlett algorithm [8, 25] that was implemented in MATLAB as the `funm` command. The Schur-Parlett algorithm consists in decomposing the matrix \mathbf{A} as \mathbf{VTV}^* (Schur decomposition [18]) and then computing the Mittag-Leffler function on the upper triangular \mathbf{T} matrix using the Taylor series and the Parlett recurrence. The derivatives for the Taylor series are calculated through a combination of series expansion, numerical inversion of the Laplace transform and summation formula. We will refer to Garrappa and Popolizio's code as `matlab`.

Note that the MATLAB backend is written in C/C++ and calls the Intel Math Kernel Library [53] for many matrix and vector operations, which exploits very efficiently the hardware resources of modern CPUs, including multi-threading and SIMD units. It is worth remarking that we only compare our code against a MATLAB implementation due to the lack of any parallel code freely available in C/C++.

Nevertheless, there are some noticeable differences between the algorithms. First of all, `matlab` only supports dense matrices and has a fixed precision (IEEE 754 double-precision standard), while ours supports both dense and sparse matrices as well as an user-defined precision. Moreover, a Monte Carlo method is not only fully parallelizable but also allows the computation of single entries of the vector solution, which is not possible with the classical deterministic algorithm. Due to the random nature of the Monte Carlo algorithms, all results reported in this section correspond to the mean values obtained after several runs. With the exception of the variance analysis, the program calculates the solution for all points in domain in all simulations.

4.2. Time-fractional diffusion equation. The first example we consider consists in solving the 2D time-fractional diffusion equation,

$$(4.1) \quad D_t^\alpha u(\mathbf{x}, t) = \nabla^2 u(\mathbf{x}, t),$$

in a domain $\Omega = [-\mu, \mu]^2$, with time $t > 0$, a space variable $\mathbf{x} = (x, y) \in \mathbb{R}^2$, an initial condition $u(\mathbf{x}, 0) = u_0(\mathbf{x})$ and a Dirichlet boundary condition $u(\mathbf{x}, t)|_{\partial\Omega} = 0$. Here D_t^α is the Caputo's fractional derivative of order α with $0 < \alpha \leq 1$. Considering a discrete mesh with m cells in each dimension, such that $\Delta x = \Delta y = 2\mu/m$, and the standard 5-point stencil finite difference approximation, the approximated solution $\hat{u}(\mathbf{x}, t)$ for (4.1) can be written as

$$(4.2) \quad \hat{u}(\mathbf{x}, t) = E_\alpha \left(\frac{m^2}{4\mu^2} \hat{\mathbf{L}} t^\alpha \right) \hat{u}_0(\mathbf{x}) = E_\alpha(\mathbf{A} t^\alpha) \hat{u}_0(\mathbf{x})$$

where $\hat{\mathbf{L}}$ denotes the discrete Laplacian operator. Here, we consider that the off-diagonal entries of $\hat{\mathbf{L}}$ are positive and the diagonal negative.

This example is particularly suited for analyzing the numerical errors since the eigenvalues of the matrix \mathbf{A} can be calculated analytically [52] and, consequently, the corresponding solution of the equation. In fact, for a point $\mathbf{x} = (x, y)$ in the discrete domain, the corresponding eigenvalue $\lambda(\mathbf{x})$ and eigenvector $\mathbf{v}(\mathbf{x})$ are known to be equal to

$$\begin{aligned} \lambda(\mathbf{x}) &= \frac{m^2}{4\mu^2} \left[2 \cos \left(\frac{x\pi}{m+1} \right) + 2 \cos \left(\frac{y\pi}{m+1} \right) - 4 \right] \\ \mathbf{v}(\mathbf{x}) &= \left\{ v_{(i,j)} = \sin \left(\frac{ix\pi}{m+1} \right) \sin \left(\frac{jy\pi}{m+1} \right) \text{ for } i, j = 1, 2, \dots, m \right\} \end{aligned}$$

After organizing the eigenvalues and eigenvectors of \mathbf{A} into the matrices \mathbf{D} and \mathbf{V} , respectively, the solution for the 2D diffusion problem can be calculated as

$$(4.3) \quad \hat{u}(\mathbf{x}, t) = \mathbf{V} E_\alpha(\mathbf{D} t^\alpha) \mathbf{V}^\top \hat{u}_0(\mathbf{x})$$

Moreover, we can determine the stiffness ratio $r = \lambda_{\max}/\lambda_{\min}$ [34] for this problem, which is given asymptotically by $r \sim 4m^2/\pi^2$ for large values of m . In particular, the diffusion problem can be considered stiff for the range of values of m used in this section and, thus, is a suitable example for testing the performance of our method in solving this class of problems.

For all the results shown in this section, we chose the domain to be $\Omega = [-1, 1]^2$ and the initial condition $\hat{u}_0(\mathbf{x}) = c m^2 \delta(\mathbf{x} - \mathbf{x}_c)$, which consists on a discrete impulse located at the center of the computational grid, $\mathbf{x}_c = (m/2, m/2)$, and strength $c = 1/4096$. Since the `matlab` code only works with dense matrices, it requires around 25GB of memory when calculating the solution for a discrete mesh with $m = 160$. In comparison, `mc_dense` uses around 10GB of memory for the same mesh, while `mc_sparse`, only a couple of megabytes. For this reason, the maximum number of cells m in any experiment will be equal to 160. Regarding the time variable t , we choose $t = 0.1$ where it is possible to clearly distinguish the diffusion process for different values of α .

Fig. 1 shows the maximum absolute error as function of the number of random paths N_p . The error has been computed using the analytical solution in (4.3). Recall

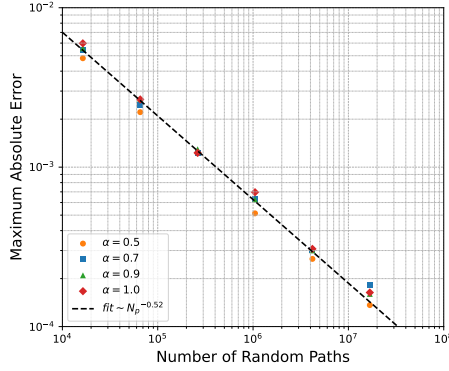


FIG. 1. Maximum absolute error as a function of the number of random paths when solving the 2D diffusion equation for $t = 0.1$ and $m = 80$.

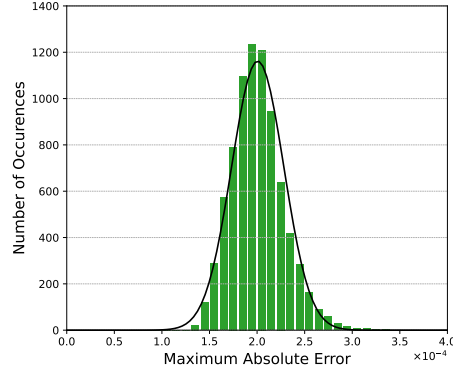


FIG. 2. A histogram of the maximum absolute error for 8000 runs, each one starting with a different random seed. In each run, we solved the 2D diffusion equation with $t = 0.1$, $m = 80$ and $N_p = 2.5 \times 10^5$.

from Section 3.2 that the numerical error of the Monte Carlo method approximates a Gaussian random variable with standard deviation determined by $\sigma N_p^{-1/2}$. This relation is confirmed numerically by the trend line in the graph, which has a slope of approximately $-1/2$ in the logarithmic scale. Repeating the Monte Carlo simulation several times with different initial seeds, we observe in Fig. 2 that the numerical errors are indeed distributed according to a normal distribution.

An estimation of the variance can be obtained for this simple initial condition, and in the limiting case when $m \gg 1$. Note that for this case there are only two possible outcomes for the random variable ω in (3.23), 0 or cm^2 , with probabilities $1 - \xi$ and ξ , respectively. The outcome cm^2 is obtained when the ending state of the random path coincides with the node of the computational mesh corresponding to the point \mathbf{x}_c , being 0 otherwise. For simplicity, let us assume that we choose the point where the solution is computed to be the same \mathbf{x}_c . Then, the outcome will be different from 0 only when, after a random number of jumps n in a random path, the final state is the same as the initial one. Estimating the probability of n is straightforward, since this problem is equivalent to the problem of computing the probability of returning to the initial point after n steps for a simple symmetric 2D random walk [28], and is given by

$$(4.4) \quad h_n = \left[\binom{n}{n/2} \frac{1}{2^n} \right]^2, \quad n = 0, 2, 4, \dots$$

Asymptotically when $n \gg 1$, $h_n \sim 2/\pi(n+1)$. Concerning the number of transitions, this is a random variable governed by a probability distribution P_n , and depends on the number of events occurring during the time interval $[0, t]$. Moreover, since the sojourn time in every state is Mittag-Leffler distributed, then the probability can be estimated, and it turns out to be the so-called fractional Poisson distribution [35],

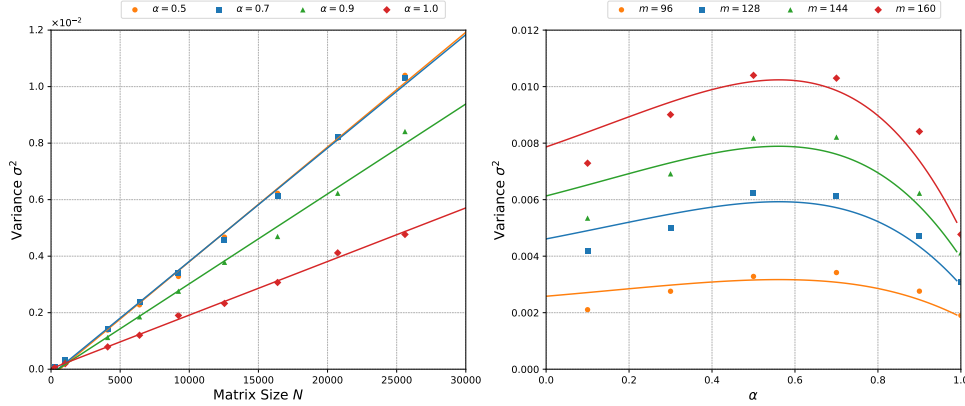


FIG. 3. Variance σ^2 of the Monte Carlo algorithm as a function of the matrix size $N = m^2$ and α when solving the 2D diffusion equation at a single point located at the centre of the mesh for $t = 0.1$. The number of random paths was kept fixed to 10^{10} .

where the mean number of events \bar{n} is

$$(4.5) \quad \bar{n} = \frac{m^2 t^\alpha}{\Gamma(\alpha + 1)},$$

and the probability of no events occurring during this time interval is $P_0 = E_\alpha(m^2 t^\alpha)$. When $m \rightarrow \infty$, a simple piecewise constant function can be used as an approximation, and yields

$$(4.6) \quad P_n \approx \begin{cases} P_0, & n \leq \frac{1}{P_0} \\ 0, & n > \frac{1}{P_0}. \end{cases}$$

Then, it follows that the probability ξ is given by

$$(4.7) \quad \xi = \sum_{n=0}^{\infty} h_{2n} P_{2n} \approx P_0 + P_0 \sum_{n=1}^{1/P_0} h_{2n}.$$

Using the known difference equation $\sum_{k=0}^{n-1} (k+x)^{-1} = \psi(x+n) - \psi(x)$, where $\psi(x)$ is the digamma function, we obtain

$$(4.8) \quad \xi \approx P_0 + \frac{P_0}{\pi} \left[\psi\left(\frac{3}{2} + \frac{1}{P_0}\right) - \psi\left(\frac{5}{2}\right) \right].$$

When $m \rightarrow \infty$, $P_0 \sim [m^2 t^\alpha \Gamma(1-\alpha)]^{-1}$, and then using the asymptotic expansion properties of the digamma function it holds that $\xi \sim [m^2 t^\alpha \Gamma(1-\alpha)]^{-1}$. Thus, asymptotically an estimation of the variance σ^2 is given by

$$(4.9) \quad \sigma^2 \sim (c m^2)^2 \xi = c^2 m^2 \frac{t^{-\alpha}}{\Gamma(1-\alpha)} = c^2 N \frac{t^{-\alpha}}{\Gamma(1-\alpha)}.$$

This relation can be seen in Fig. 3. For a fixed α and t , the variance σ^2 scales linearly with the matrix size $N = m^2$. Likewise, for a fixed N , t , the variance σ^2 is

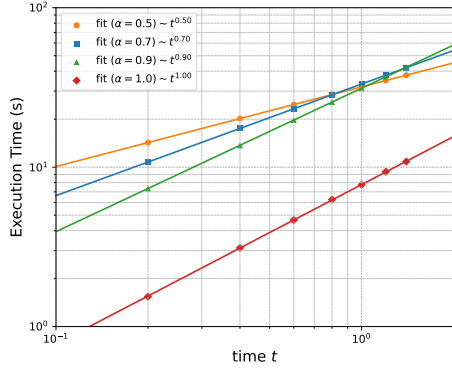


FIG. 4. Elapsed time for solving the 2D diffusion equation as a function of the time t and the parameter α for $m = 80$. The number of random paths was kept fixed at 10^5 .

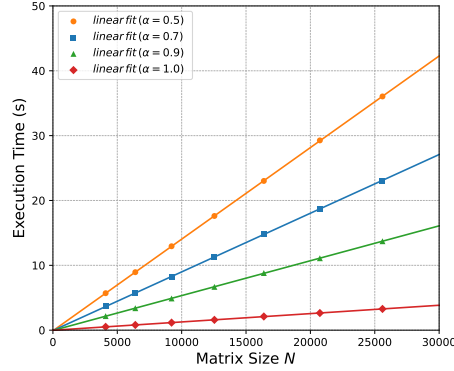


FIG. 5. Elapsed time for solving the 2D diffusion equation as a function of the matrix size $N = m^2$ and the parameter α for $t = 0.1$. The number of random paths was kept fixed at 10^6 .

proportional to $[t^\alpha \Gamma(1 - \alpha)]^{-1}$. Note that the points in the graph do not perfectly match the curve from (4.9) due to the low number of cells m used in the simulation. Still, it provides the best approximation for the variance σ^2 under these conditions.

Concerning the computational cost of the Monte Carlo algorithm, this depends on the number of random paths and the time for generating each path. Even though this time is random, we can readily assume to be proportional to the mean time of events in (4.5). Therefore, the computational cost of the algorithm is of the order of $O(N_p N t^\alpha)$, which is in good agreement with the results shown in Fig. 4 and 5. For a fixed number of random paths N_p and matrix size N , the execution time is proportional to t^α as shown in Fig. 4. Note that the scale is $\log - \log$ and the slope of the curves coincides with α . Similarly, when we kept fixed both the time t and number of random paths N_p , the execution time grows linearly with the matrix size N as shown in Fig. 5. It is worth mentioning that exponential random numbers are much cheaper to produce than ML random numbers, resulting in significantly lower execution times when $\alpha = 1$.

To compare the performance and scaling of our methods against a classical approach, we measure the serial and parallel execution times for different matrix sizes $N = m^2$ as shown in Fig. 6. In terms of execution time, the Monte Carlo algorithm is several times faster than the `matlab` code, especially when fully exploiting the sparse nature of the problem, while maintaining a reasonable precision (*i.e.*, the maximum error in any simulation is below 3×10^{-4}). When using 8 threads and considering a discrete mesh with $m = 128$, both `matlab` and `mc_dense` shows a speedup of 6.5 (or an efficiency of 81.25%), while `mc_sparse` presents a speedup of 7.5 (95% efficiency).

Since matrix \mathbf{A} is real and symmetric, its Schur decomposition can be written as $\mathbf{A} = \mathbf{V}\mathbf{D}\mathbf{V}^\top$, where \mathbf{D} is a diagonal matrix containing the eigenvalues of \mathbf{A} , and the columns of the matrix \mathbf{V} the corresponding eigenvectors. In this case, the matrix function $f(\mathbf{A})$ can be simply evaluated as $f(\mathbf{A}) = \mathbf{V}f(\mathbf{D})\mathbf{V}^\top$ [8]. MATLAB uses a QR algorithm to compute the Schur decomposition, directly calling the corresponding routine from the Intel Math Kernel Library (*e.g.*, `dsteqr` for real symmetric matrices). The QR algorithm has a well-known computational complexity of order $O(N^3)$.

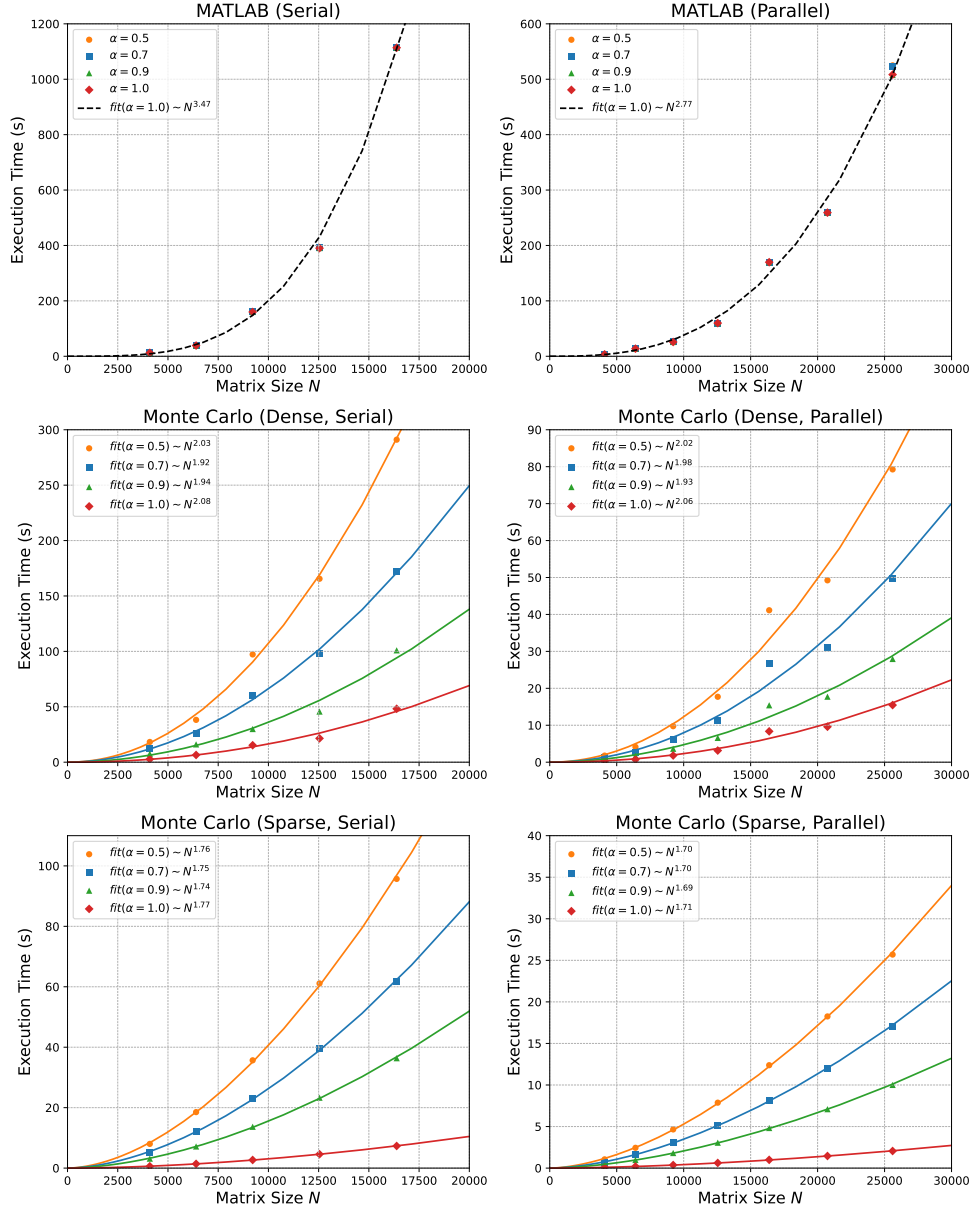


FIG. 6. Serial (left) and parallel with 8 threads (right) execution times for solving the 2D diffusion equation as a function of the matrix size $N = m^2$ for $t = 0.1$. For the Monte Carlo algorithms, the accuracy ϵ was kept fixed at 3×10^{-4} .

In comparison, the Monte Carlo algorithm requires an order of $O(N^2)$ operations to solve the diffusion equation, as shown in Fig. 6. Considering that the variance σ^2 and, consequently, the statistical error grow with the matrix size N , the number of random paths must increase proportionally to the matrix size in order to keep the same level of accuracy for the numerical solution.

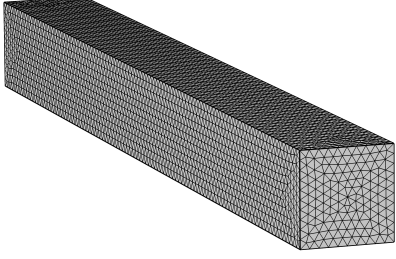


FIG. 7. Computational mesh of the domain where the fractional convection-diffusion equation is solved.

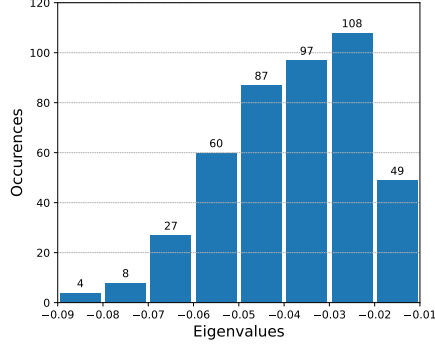


FIG. 8. Histogram of the eigenvalues of $\mathbf{A} = \mathbf{B}^{-1}\mathbf{K}$ from (4.13). Here the scale parameter was set to $s = 30$, which results in a matrix of size $N = 453$.

4.3. Time-fractional convection-diffusion equation. The second example we discuss in this paper consists in solving a time-fractional convection-diffusion equation:

$$(4.10) \quad D_t^\alpha u(\mathbf{x}, t) = c \nabla^2 u(\mathbf{x}, t) + \nu \nabla u(\mathbf{x}, t)$$

with boundary and initial conditions, respectively

$$(4.11) \quad u(\mathbf{x}, t)|_{\partial\Omega} = g(\mathbf{x}, t) \quad u(\mathbf{x}, 0) = f(\mathbf{x})$$

where c is the diffusion coefficient and ν the velocity field. After applying the standard Galerkin finite element method [55] to the discretized nodes x_i for $i = 0, 1, \dots, n$, we obtain the following system of equations:

$$(4.12) \quad \mathbf{B} D_t^\alpha \mathbf{u} = \mathbf{K} \mathbf{u} + \mathbf{h}, \quad \mathbf{u}(0) = \mathbf{u}_0$$

where $\mathbf{u} = \{u(x_1, t), u(x_2, t), \dots, u(x_n, t)\}$, \mathbf{B} is the assembled mass matrix, \mathbf{K} is the corresponding assembled stiffness matrix and \mathbf{h} is the load vector. The diffusion coefficient c , the velocity field ν , and the boundary conditions are already included in these matrices and vector. To simplify the computation, the mass matrix was lumped [55], transforming the mass matrix into a diagonal matrix.

The solution for the inhomogeneous systems of fPDEs in (4.12) can be written in terms of the Mittag-Leffler function as follows

$$(4.13) \quad \mathbf{u}(\mathbf{x}, t) = E_\alpha(\mathbf{A} t^\alpha) \mathbf{u}_0(\mathbf{x}) + \int_0^t ds (t-s)^{\alpha-1} E_\alpha(\mathbf{A} (t-s)^\alpha) \mathbf{v}$$

with $\mathbf{A} = \mathbf{B}^{-1}\mathbf{K}$ and $\mathbf{v} = \mathbf{B}^{-1}\mathbf{h}$. Note that the second term in the right side depends on the boundary data, and in particular for numerical purpose it will require to approximate a definite integral. This will entail another source of error along with the aforementioned statistical error. Since the goal of this manuscript is to focus solely on computing numerically the ML function, and analyzing the associated statistical error,

TABLE 1

The execution time of the `matlab` code for computing the solution of the 3D convection-diffusion equation for different values of t and α considering a scale parameter $s = 30$ (the total number of nodes in the computational mesh was 453). The parameters of `funm` were kept at their default values. The number in parenthesis indicates the order of the derivative of the largest block.

	$\alpha = 1$	$\alpha = 0.9$	$\alpha = 0.7$	$\alpha = 0.5$
$t = 20$	6.43 (19)	FAIL	FAIL	919 (21)
$t = 40$	5.81 (22)	FAIL	FAIL	965 (24)
$t = 60$	5.55 (24)	FAIL	FAIL	967 (24)
$t = 80$	6.15 (27)	FAIL	FAIL	971 (25)
$t = 100$	6.78 (30)	FAIL	FAIL	982 (27)

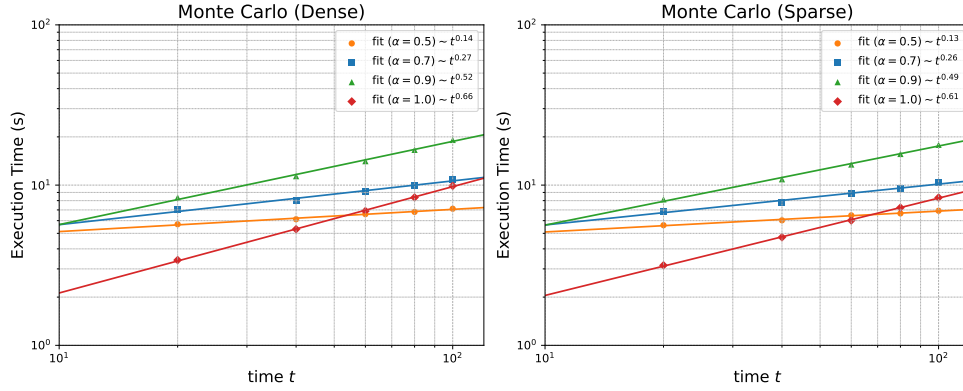


FIG. 9. Serial execution time of the probabilistic algorithm for computing the solution of the 3D convection-diffusion equation for different values of t and α , considering a scale parameter $s = 30$ (the total number of nodes in the computational mesh was 453). The number of random paths was kept fixed at 10^8 , resulting in a precision $\epsilon \approx 10^{-4}$.

here we set a null value for the Dirichlet boundary conditions $f(\mathbf{x}) = 0$, and hence $\mathbf{h} = 0$. Clearly the general case deserves further investigation, a detailed analysis is left for a future manuscript.

For the domain, we consider here a block of aluminium of $2s \times 2s \times 20s$ ($W \times H \times L$, in cm) with a scale parameter s , an isotropic diffusion coefficient $c = 9.4 \times 10^{-5} \text{ m}^2/\text{s}$ [46], a field velocity $\nu = 0$ and a Dirichlet boundary condition $u = 0$ on the surface of the block. The finite-element mesh in Fig. 7 was generated using the scientific application tool *COMSOL* [1] considering a maximum and minimum element size equal to 20 cm and 0.1 cm, respectively. Based on this mesh, we generated the corresponding finite-element method (FEM) matrices and vectors. For the initial conditions we use again a discrete impulse located at the position $(s, s, 10s)$. It is worth mentioning that the resulting matrix is asymmetric, having entries entirely arbitrary in both sign and magnitude, and in this sense this can be considered as a much more complex example than the case analysed in the previous section.

Similarly to the previous example, we examine the eigenvalues of matrix \mathbf{A} to gain some insight about its numerical properties. In this case, the eigenvalues were

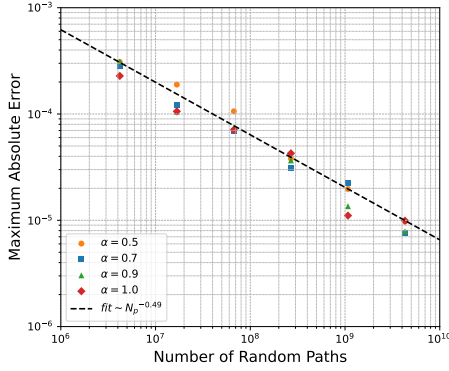


FIG. 10. Maximum absolute error of the `mc_sparse` algorithm as a function of the number of random paths when solving the 3D convection-diffusion equation for time $t = 40$ and scale parameter $s = 100$ (the total number of nodes in the computational mesh was 25120).

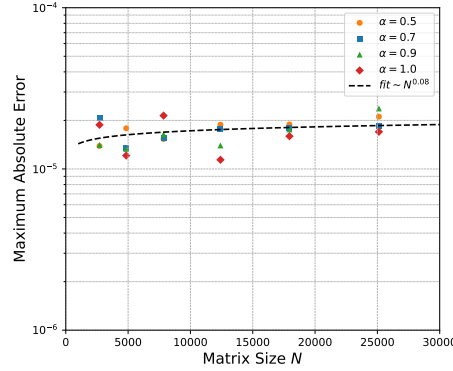


FIG. 11. Maximum absolute error of the `mc_sparse` algorithm as a function of the number of nodes N in the computational mesh when solving the 3D convection-diffusion equation for $t = 40$. The number of random paths was kept fixed at 10^9 .

calculated through the command `eigs` of MATLAB, which corresponds in essence to the Arnoldi method. Fig. 8 depicts the histogram for the eigenvalues of the matrix \mathbf{A} . The eigenvalues are not only small but are also highly clustered between -0.02 and -0.05 , which is a problem for the `matlab` code of [17]. On one hand, this leads to very large blocks during the partitioning of the Schur form of \mathbf{A} in the Schur-Parlett algorithm [8, 17]. The evaluation of the Taylor series is particularly expensive for large blocks since it requires order $O(m^4)$ operations, where m is the size of the block. On the other hand, the numerical evaluation of high-order derivatives of the Mittag-Leffler function often entails very large numbers even for small input values due to the rapidly increasing factorial $(x)_k = x(x-1)\dots(x-k+1)$:

$$(4.14) \quad \frac{d^k}{dz^k} E_\alpha(z) = \sum_{j=k}^{\infty} \frac{(j)_k}{\Gamma(\alpha j + 1)} z^{j-k}, \quad k \in \mathbb{N}$$

Indeed, MATLAB reports an infinite derivative when trying to compute the ML function for $\alpha = 0.7$ and the algorithm fails to converge to a solution for $\alpha = 0.9$ even after computing 250 terms of the Taylor series. This is shown in Table 1. The `matlab` algorithm was able to reach a solution for $\alpha = 0.5$ and $\alpha = 1$.

In the Schur-Parlett algorithm, the Schur form of \mathbf{A} are divided into blocks according to its eigenvalues. In particular, if the absolute difference between two eigenvalues is less than a tolerance δ , they will be assigned to the same block. With the default tolerance $\delta = 0.1$, almost all eigenvalues of \mathbf{A} will be grouped into a single, large block. Even after decreasing the tolerance to $\delta = 0.01$, most eigenvalues are still concentrated into a single block. Note that the value of δ cannot be too small, otherwise the two distinct blocks may contain close eigenvalues, causing the Parlett's recurrence to break down due to numerical cancellations [8, 24]. It is worth mentioning that the derivatives of the ML function are calculated serially and, thus, the `matlab` code shows very little speedup when using multiple threads.

Concerning the computational cost of the Monte Carlo method for solving this problem, recall that this depends on the number of random paths and the mean

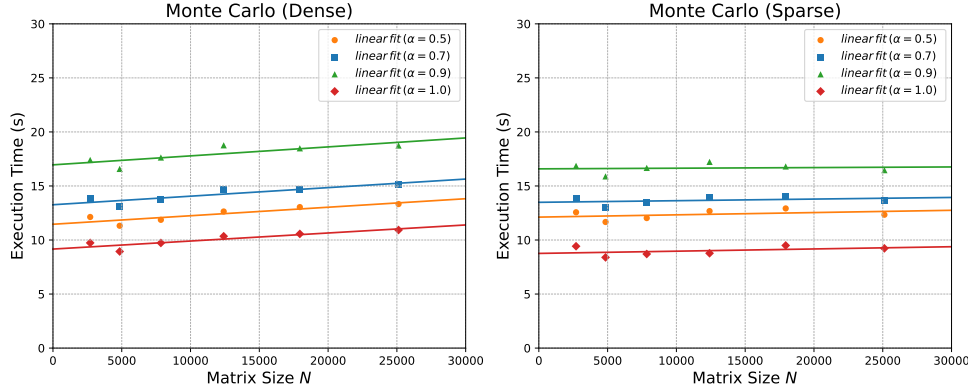


FIG. 12. Parallel execution time of the Monte Carlo method as a function of the number of nodes N in the computational mesh when computing the solution of the 3D convection-diffusion equation for $t = 40$. The number of random paths was kept fixed at 10^9 , resulting in an error $\epsilon \approx 2 \times 10^{-5}$.

number of events occurred during the prescribed time interval. The former is chosen according to the desired level of accuracy for the numerical solution. As it was already explained for the previous example, the numerical error depends not only on the number of random paths but also on the variance, which depends on the specific entries of the matrix \mathbf{A} and the input vector \mathbf{u} . The more heterogeneous they are, the larger the variance will be, and consequently more random paths will be required for attaining the prescribed accuracy. Regarding the mean number of events, this depends on the specific values of the diagonal entries of \mathbf{A} , being larger for larger entries.

In contrast to the `matlab` code which depends strongly on the distribution of eigenvalues, the Monte Carlo method do not show explicit dependency on them. For this reason, the stochastic method was able to compute the solution regardless of the values of t or α . The execution time of `mc_dense` and `mc_sparse` for different values of t and α are shown in Fig. 9. Regarding the parallel performance, `mc_dense` and `mc_sparse` usually achieve a speedup between 5 and 6 when using 8 threads.

Figures 10 and 11 show the maximum absolute error as a function of the number of random paths and the matrix size N , respectively. Note that the numerical error of the method ϵ decreases with the square root of the number of random paths as theoretically expected.

In the previous example, the domain was fixed to $\Omega = [-1, 1]^2$, and the matrix size was enlarged increasing the number of grid points inside the domain. As a result the magnitude of the diagonal entries of the matrix increases accordingly, and so do the mean number of events and the variance. We now consider a case where the distance between two nodes in the finite-element mesh was kept constant when the domain is conveniently scaled in order to increase the matrix size. This leads to a matrix with diagonal entries independent of the matrix size, and therefore, the execution time and error of the Monte Carlo algorithm only depend on the number of random paths. This is shown in Fig. 11 and 12. Note however that the algorithm needs to perform a binary search for selecting the next state of the random path, which causes the execution time to slightly grow as the matrix size increases. This

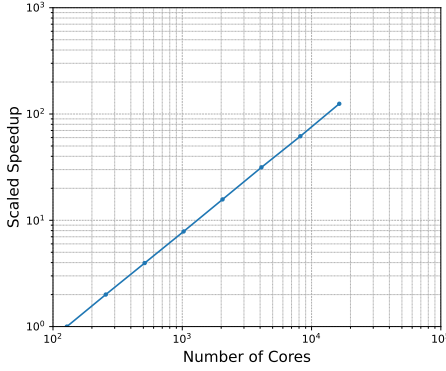


FIG. 13. Weak scaling of `mc_sparse` in the Karolina supercomputer. This test solves a 2D diffusion equation for $t = 0.1$, $\mu = 1$ and $m = 1024$ ($N = m^2 = 1,048,576$). The number of random paths was chosen based on the number of cores, beginning with 2×10^6 .

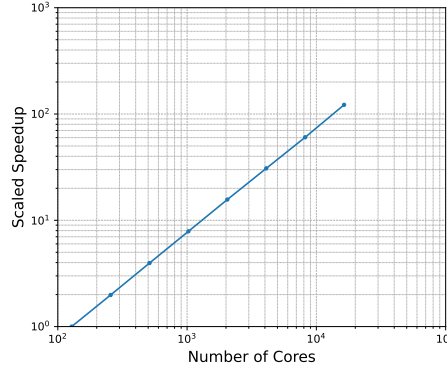


FIG. 14. Weak scaling of `mc_sparse` in the Karolina supercomputer. This test solves a 3D convection-diffusion equation for $t = 40$ considering a scalar parameter $s = 300$ (the total number of nodes in the computational mesh was 753,675). The number of random paths was chosen based on the number of cores, beginning with 10^{11} .

has a negligible effect on the sparse implementation due to a low number of nonzero entries per matrix row.

4.4. Distributed-Memory Performance. The distributed-memory tests were carried out at the Karolina Supercomputer located in IT4Innovations National Supercomputing Centre. Each computational node in the cluster contains two AMD 7H12 64C @2.6GHz CPUs and 256GB of RAM, running CentOS 7. For all tests, two MPI processes were launched on each node (one per processor) with as many threads as the number of physical cores (64). Since there is no freely available code capable of computing the action of a Mittag-Leffler function over a vector that is suitable for distributed-memory systems, this section only contains the results for the Monte Carlo method (`mc_sparse`). The C++ code was compiled with GCC 12.1.0 and OpenMPI 4.1.4 with the `-O3` and `-march=native` flags.

Figures 13 and 14 show the weak scaling of `mc_sparse` between 1 and 128 nodes (16,384 cores), considering a single computational node as the baseline. While the scaling of the domain size is typically used to increase the workload, for the specific FEM problem in (4.12), as it was shown in the previous section, this does not affect the computational time, and therefore does not provide any useful insight about the scalability of the algorithm. Instead, we increased the workload by scaling the number of random paths according with the number of nodes used. In doing so the statistical error reduces, improving the accuracy of the computed solution.

Since all random paths in the Monte Carlo method are independent, the task of generating them can be done in parallel and the parallel code only needs to communicate at the end of the simulation to combine the results. This is the reason that the `mc_sparse` shows perfect scalability in both examples.

5. Conclusion. In this paper we propose a novel stochastic method for solving time fractional partial differential equations. These equations are already being used for modeling natural phenomenon subject to memory effects, and microscopi-

cally are typically described by non-Markovian processes. Fractional equations are capable of capturing such effects due to the inherent non-locality of the operator. As a consequence, the classical numerical schemes often based on time-stepping suffer from heavy memory storage requirements since the numerical solution of the fPDEs at current time depends on all preceding time instances. This can be even worse when dealing with high-dimensional problems, degrading significantly the performance of the corresponding numerical algorithms.

The main advantage of the proposed method rests on the fact that it allows for the computation of the solution at single point of a given domain, or equivalently a single entry of the corresponding vector solution. Moreover, the numerical algorithm is not based on any time-stepping scheme, and therefore the solution is obtained without the need of storing previous results. Rather, the solution is computed through an expected value of a functional of random processes which resembles the non-Markovian process found in the microscopic description of the phenomenon, and hence exploits somehow naturally the non-locality of the fractional operators.

Furthermore, since the method is based on Monte Carlo it inherits all the known advantages from a computational point of view, such as the comparative ease of implementation in parallel, fault-tolerance, and in general of being well suited for heterogeneous architectures. In fact, our parallel implementation was able to solve large-scale problems efficiently in both shared-memory and distributed-memory systems, demonstrating the versatility and scalability of the probabilistic method compared to the classical numerical schemes.

REFERENCES

- [1] *COMSOL: Multiphysics Software for Optimizing Designs*. <https://www.comsol.com/>.
- [2] J. ACEBRÓN, *A Monte Carlo method for computing the action of a matrix exponential on a vector*, Applied Mathematics and Computation, 362 (2019), p. 124545, <https://doi.org/10.1016/j.amc.2019.06.059>.
- [3] J. A. ACEBRÓN, J. R. HERRERO, AND J. MONTEIRO, *A highly parallel algorithm for computing the action of a matrix exponential on a vector based on a multilevel Monte Carlo method*, Computers & Mathematics with Applications, 79 (2020), pp. 3495–3515, <https://doi.org/10.1016/j.camwa.2020.02.013>.
- [4] F. ARRIGO AND F. DURASTANTE, *Mittag-Leffler Functions and their Applications in Network Science*, SIAM Journal on Matrix Analysis and Applications, 42 (2021), pp. 1581–1601, <https://doi.org/10.1137/21M1407276>.
- [5] M. BENZI, T. M. EVANS, S. P. HAMILTON, M. LUPO PASINI, AND S. R. SLATTERY, *Analysis of Monte Carlo accelerated iterative methods for sparse linear systems*, Numerical Linear Algebra with Applications, 24 (2017), <https://doi.org/10.1002/nla.2088>.
- [6] A. C. BERRY, *The Accuracy of the Gaussian Approximation to the Sum of Independent Variates*, Transactions of the American Mathematical Society, 49 (1941), pp. 122–136, <https://doi.org/10.2307/1990053>, <https://arxiv.org/abs/1990053>.
- [7] Y. CHEN, I. PETRAS, AND D. XUE, *Fractional order control - A tutorial*, in 2009 American Control Conference, June 2009, pp. 1397–1411, <https://doi.org/10.1109/ACC.2009.5160719>.
- [8] P. I. DAVIES AND N. J. HIGHAM, *A Schur-Parlett Algorithm for Computing Matrix Functions*, SIAM Journal On Matrix Analysis and Applications, 25 (2003), pp. 464–485, <https://doi.org/10.1137/S0895479802410815>.
- [9] L. DEVROYE, *Non-Uniform Random Variate Generation*, Springer, New York, first ed., 1986.
- [10] I. DIMOV, *Monte Carlo Methods for Applied Scientists*, World Scientific, Singapore, 2008.
- [11] I. DIMOV, V. ALEXANDROV, AND A. KARAVANOVA, *Parallel resolvent Monte Carlo algorithms for linear algebra problems*, Mathematics and Computers in Simulation, 55 (2001), pp. 25–35, [https://doi.org/10.1016/S0378-4754\(00\)00243-3](https://doi.org/10.1016/S0378-4754(00)00243-3).
- [12] I. DIMOV, S. MAIRE, AND J. M. SELLIER, *A new Walk on Equations Monte Carlo method for solving systems of linear algebraic equations*, Applied Mathematical Modelling, 39 (2015), pp. 4494–4510, <https://doi.org/10.1016/j.apm.2014.12.018>.

- [13] E. ESTRADA, *Fractional diffusion on the human proteome as an alternative to the multi-organ damage of SARS-CoV-2*, *Chaos: An Interdisciplinary Journal of Nonlinear Science*, 30 (2020), p. 081104, <https://doi.org/10.1063/5.0015626>.
- [14] G. E. FORSYTHE AND R. A. LEIBLER, *Matrix Inversion by a Monte Carlo Method*, *Mathematical Tables and Other Aids to Computation*, 4 (1950), pp. 127–129, <https://doi.org/10.2307/2002508>, <https://arxiv.org/abs/2002508>.
- [15] D. FULGER, E. SCALAS, AND G. GERMANO, *Random numbers from the tails of probability distributions using the transformation method*, *Fractional Calculus and Applied Analysis*, 16 (2013), pp. 332–353, <https://doi.org/10.2478/s13540-013-0021-z>.
- [16] R. GARRAPPA, *Numerical Evaluation of Two and Three Parameter Mittag-Leffler Functions*, *SIAM Journal on Numerical Analysis*, 53 (2015), pp. 1350–1369, <https://doi.org/10.1137/140971191>.
- [17] R. GARRAPPA AND M. POPOLIZIO, *Computing the matrix Mittag-Leffler function with applications to fractional calculus*, *Journal of Scientific Computing*, 77 (2018), pp. 129–153, <https://doi.org/10.1007/s10915-018-0699-5>, <https://arxiv.org/abs/1804.04883>.
- [18] G. H. GOLUB AND C. F. VAN LOAN, *Matrix Computations*, Johns Hopkins Studies in the Mathematical Sciences, The Johns Hopkins University Press, Baltimore, MD, fourth ed., 2013.
- [19] R. GORENFLO, A. A. KILBAS, F. MAINARDI, AND S. ROGOSIN, *Mittag-Leffler Functions, Related Topics and Applications*, Springer Monographs in Mathematics, Springer Berlin Heidelberg, Berlin, Heidelberg, 2020, <https://doi.org/10.1007/978-3-662-61550-8>.
- [20] R. GORENFLO, J. LOUTCHKO, AND Y. LUCHKO, *Computation of the Mittag-Leffler function and its derivatives*, *Fractional Calculus & Applied Analysis (FCAA)*, 5 (2002), pp. 491–518.
- [21] R. GORENFLO AND F. MAINARDI, *Fractional Calculus*, in *Fractals and Fractional Calculus in Continuum Mechanics*, A. Carpinteri and F. Mainardi, eds., International Centre for Mechanical Sciences, Springer, Vienna, 1997, pp. 223–276.
- [22] B. GUO, X. PU, AND F. HUANG, *Fractional Partial Differential Equations And Their Numerical Solutions*, World Scientific, Singapore, Mar. 2015.
- [23] C. R. HARRIS, K. J. MILLMAN, S. J. VAN DER WALT, R. GOMMERS, P. VIRTANEN, D. COUNAPEAU, E. WIESER, J. TAYLOR, S. BERG, N. J. SMITH, R. KERN, M. PICUS, S. HOYER, M. H. VAN KERKWIJK, M. BRETT, A. HALDANE, J. F. DEL RÍO, M. WIEBE, P. PETERSON, P. GÉRARD-MARCHANT, K. SHEPPARD, T. REDDY, W. WECKESSER, H. ABBASI, C. GOHLKE, AND T. E. OLIPHANT, *Array programming with NumPy*, *Nature*, 585 (2020), pp. 357–362, <https://doi.org/10.1038/s41586-020-2649-2>.
- [24] N. J. HIGHAM, *Accuracy and Stability of Numerical Algorithms*, Other Titles in Applied Mathematics, Society for Industrial and Applied Mathematics, Philadelphia, PA, second ed., Jan. 2002.
- [25] N. J. HIGHAM, *Functions of Matrices*, Other Titles in Applied Mathematics, Society for Industrial and Applied Mathematics, Philadelphia, PA, Jan. 2008, <https://doi.org/10.1137/1.9780898717778>.
- [26] R. HILFER, *Applications Of Fractional Calculus In Physics*, World Scientific, Singapore, Mar. 2000.
- [27] R. HILFER AND H. J. SEYBOLD, *Computation of the generalized Mittag-Leffler function and its inverse in the complex plane*, *Integral Transforms and Special Functions*, 17 (2006), pp. 637–652, <https://doi.org/10.1080/10652460600725341>.
- [28] O. C. IBE, *Elements of Random Walk and Diffusion Processes*, John Wiley & Sons, Sept. 2013.
- [29] H. JI, M. MASCAGNI, AND Y. LI, *Convergence Analysis of Markov Chain Monte Carlo Linear Solvers Using Ulam-Von Neumann Algorithm*, *SIAM Journal on Numerical Analysis*, 51 (2013), pp. 2107–2122, <https://arxiv.org/abs/42004066>.
- [30] T. J. KOZUBOWSKI, *Computer simulation of geometric stable distributions*, *Journal of Computational and Applied Mathematics*, 116 (2000), pp. 221–229, [https://doi.org/10.1016/S0377-0427\(99\)00318-0](https://doi.org/10.1016/S0377-0427(99)00318-0).
- [31] T. J. KOZUBOWSKI, *Exponential Mixture Representation of Geometric Stable Distributions*, *Annals of the Institute of Statistical Mathematics*, 52 (2000), pp. 231–238, <https://doi.org/10.1023/A:1004157620644>.
- [32] T. J. KOZUBOWSKI, *Fractional moment estimation of linnik and mittag-leffler parameters*, *Mathematical and Computer Modelling*, 34 (2001), pp. 1023–1035, [https://doi.org/10.1016/S0895-7177\(01\)00115-7](https://doi.org/10.1016/S0895-7177(01)00115-7).
- [33] T. J. KOZUBOWSKI AND S. T. RACHEV, *Univariate Geometric Stable Laws*, *Journal of Computational Analysis and Applications*, 1 (1999), pp. 177–217, <https://doi.org/10.1023/A:1022629726024>.

- [34] J. D. LAMBERT, *Computational Methods in Ordinary Differential Equations*, vol. Vol. 5, John Wiley & Sons Incorporated, New York, Feb. 1973.
- [35] N. LASKIN, *Fractional Poisson process*, Communications in Nonlinear Science and Numerical Simulation, 8 (2003), pp. 201–213, [https://doi.org/10.1016/S1007-5704\(03\)00037-6](https://doi.org/10.1016/S1007-5704(03)00037-6).
- [36] A. LISCHKE, G. PANG, M. GULIAN, F. SONG, C. GLUSA, X. ZHENG, Z. MAO, W. CAI, M. M. MEERSCHAERT, M. AINSWORTH, AND G. E. KARNIADAKIS, *What is the fractional Laplacian? A comparative review with new results*, Journal of Computational Physics, 404 (2020), p. 109009, <https://doi.org/10.1016/j.jcp.2019.109009>.
- [37] R. MAGIN, *Fractional Calculus in Bioengineering, Part 1*, Critical Reviews™ in Biomedical Engineering, 32 (2004), <https://doi.org/10.1615/CritRevBiomedEng.v32.i1.10>.
- [38] F. MAINARDI, *Fractional Calculus And Waves In Linear Viscoelasticity: An Introduction To Mathematical Models*, World Scientific, London, May 2010.
- [39] F. MAINARDI, *Why the Mittag-Leffler Function Can Be Considered the Queen Function of the Fractional Calculus?*, Entropy, 22 (2020), p. 1359, <https://doi.org/10.3390/e22121359>.
- [40] G. MARSAGLIA AND W. W. TSANG, *The Ziggurat Method for Generating Random Variables*, Journal of Statistical Software, 5 (2000), <https://doi.org/10.18637/jss.v005.i08>.
- [41] J. H. MARTÍNEZ, S. ROMERO, J. J. RAMASCO, AND E. ESTRADA, *The world-wide waste web*, Nature Communications, 13 (2022), p. 1615, <https://doi.org/10.1038/s41467-022-28810-x>.
- [42] R. METZLER AND J. KLAFTER, *The random walk's guide to anomalous diffusion: A fractional dynamics approach*, Physics Reports, 339 (2000), pp. 1–77, [https://doi.org/10.1016/S0370-1573\(00\)00070-3](https://doi.org/10.1016/S0370-1573(00)00070-3).
- [43] I. MORET AND P. NOVATI, *On the Convergence of Krylov Subspace Methods for Matrix Mittag-Leffler Functions*, SIAM Journal on Numerical Analysis, 49 (2011), pp. 2144–2164, <https://doi.org/10.1137/080738374>.
- [44] J. A. NICHOLS, B. I. HENRY, AND C. N. ANGSTMANN, *Subdiffusive discrete time random walks via Monte Carlo and subordination*, Journal of Computational Physics, 372 (2018), pp. 373–384, <https://doi.org/10.1016/j.jcp.2018.06.044>.
- [45] M. E. O'NEILL, *PCG: A Family of Simple Fast Space-Efficient Statistically Good Algorithms for Random Number Generation*, Tech. Report HMC-CS-2014-0905, Harvey Mudd College, Claremont, CA, Sept. 2014.
- [46] W. J. PARKER, R. J. JENKINS, C. P. BUTLER, AND G. L. ABBOTT, *Flash Method of Determining Thermal Diffusivity, Heat Capacity, and Thermal Conductivity*, Journal of Applied Physics, 32 (1961), pp. 1679–1684, <https://doi.org/10.1063/1.1728417>.
- [47] R. N. PILLAI, *On Mittag-Leffler functions and related distributions*, Annals of the Institute of Statistical Mathematics, 42 (1990), pp. 157–161, <https://doi.org/10.1007/BF00050786>.
- [48] H. RUBIN AND B. C. JOHNSON, *Efficient generation of exponential and normal deviates*, Journal of Statistical Computation and Simulation, 76 (2006), pp. 509–518, <https://doi.org/10.1080/10629360500108004>.
- [49] J. SABATIER, O. P. AGRAWAL, AND J. A. TENREIRO MACHADO, eds., *Advances in Fractional Calculus: Theoretical Developments and Applications in Physics and Engineering*, Springer, Dordrecht, 2007.
- [50] W. E. SCHIESSER, *The Numerical Method of Lines: Integration of Partial Differential Equations*, Elsevier, San Diego, CA, 1st ed., June 1991.
- [51] H. SEYBOLD AND R. HILFER, *Numerical Algorithm for Calculating the Generalized Mittag-Leffler Function*, SIAM Journal on Numerical Analysis, 47 (2009), pp. 69–88, <https://doi.org/10.1137/070700280>.
- [52] G. STRANG, *Computational Science and Engineering*, Wellesley-Cambridge Press, Wellesley, MA, Nov. 2007.
- [53] E. WANG, Q. ZHANG, B. SHEN, G. ZHANG, X. LU, Q. WU, AND Y. WANG, *Intel Math Kernel Library*, in High-Performance Computing on the Intel® Xeon Phi™: How to Fully Exploit MIC Architectures, E. Wang, Q. Zhang, B. Shen, G. Zhang, X. Lu, Q. Wu, and Y. Wang, eds., Springer International Publishing, Cham, 2014, pp. 167–188.
- [54] B. J. WEST, *Fractional Calculus View of Complexity: Tomorrow's Science*, CRC Press, Boca Raton, FL, Jan. 2016.
- [55] O. C. ZIENKIEWICZ, R. L. TAYLOR, AND J. Z. ZHU, *The Finite Element Method: Its Basis and Fundamentals*, Elsevier, Kidlington, Oxford, seventh ed., Aug. 2013.